Available online at www.sciencedirect.com

ScienceDirect

journal homepage: www.elsevier.com/locate/he

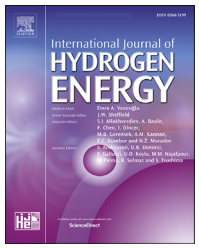

Direct electrification of Rh/Al_2O_3 washcoated SiSiC foams for methane steam reforming: An experimental and modelling study

Lei Zheng [1], *Matteo Ambrosetti* [1], *Francesca Zaio*, *Alessandra Beretta*, *Gianpiero Groppi*, *Enrico Tronconi* [*]

Laboratory of Catalysis and Catalytic Processes, Dipartimento di Energia, Politecnico di Milano, Via Lambruschini 4, 20156, Milano, Italy

HIGHLIGHTS

- Methane steam reforming via direct Joule heating of Rh/Al_2O_3 washcoated SiSiC foam.
- High space velocities increase H_2 productivity and overall energy efficiency.
- A predictive mathematical model shows excellent agreement with the experiments.
- Scale up calculations promise compact eMSR units with high H_2 productivities.

ARTICLE INFO

Article history:
Received 15 August 2022
Received in revised form
30 November 2022
Accepted 29 December 2022
Available online 19 January 2023

Keywords:
Electrified methane steam reforming
Hydrogen production
Decarbonization
Structured catalysts
Process intensification

ABSTRACT

Electrified methane steam reforming (eMSR) is a promising concept for low-carbon hydrogen production. We investigate an innovative eMSR reactor where SiSiC foams, coated with Rh/Al_2O_3 catalyst, act as electrical resistances to generate the reaction heat via the Joule effect. The novel system was studied at different temperatures, space velocities, operating pressures and catalyst loadings. Thanks to efficient heating, active catalyst and optimal substrate geometry, complete methane conversions were observed even at a high space velocity of 200000 $Nl/h/kg_{cat}$. A specific energy demand as low as 1.24 kWh/Nm^3_{H2}, with an unprecedented energy efficiency of 81%, was achieved on a washcoated foam with catalyst density of 86.3 g/L (GHSV = 150000 $Nl/h/kg_{cat}$, S/C = 4.1, ambient pressure). A mathematical model was validated against measured performance indicators and used to design an intensified eMSR unit for small scale H_2 production.

Introduction

Due to its high versatility as an energy carrier, hydrogen will play a relevant role to enabling greater penetration of renewables into the power generation sectors, and in general towards decarbonization [1,2]. Hydrogen represents a valid and cleaner alternative to fossil fuels since its use does not lead to the release of greenhouse gas at the end-use point. Hydrogen traditionally has been used as feedstocks for oil

* *Corresponding author.*
E-mail address: enrico.tronconi@polimi.it (E. Tronconi).
[1] These authors contributed equally.

https://doi.org/10.1016/j.ijhydene.2022.12.346

refining and chemical synthesis, such as ammonia and methanol. The global demand for hydrogen reached the value of almost 90 Mtons in 2020, mostly devoted to chemical uses, however the trend shows a constant growth during previous years, as suggested by International Energy Agency (IEA) outlook [3].

Methane steam reforming (MSR) is currently the most widespread process for hydrogen generation and accounts for more than half of its global production [4,5]. The hydrogen production is governed by the methane reforming reaction (Eq. (1)) and water-gas shift reaction (WGS, Eq. (2)) [6,7]. The process is globally endothermic.

$$CH_4 + H_2O \rightleftharpoons CO + 3H_2 \qquad \Delta H_r^\circ = 206\ kJ/mol \tag{1}$$

$$CO + H_2O \rightleftharpoons CO_2 + H_2 \qquad \Delta H_r^\circ = -41\ kJ/mol \tag{2}$$

Industrial-scale MSR is typically operated in multi-tubular reactors (10–14 m long, ~10 cm in diameter) with high flow rates, in order to maximize heat transfer between the catalyst pellets (typically Ni-based catalysts) and the reactor tubes [2,8]. The process runs at pressures up to 30 bar and temperatures in excess of 900°C to favor methane conversion. The heat of the reaction is provided by fuel combustion, *i.e.*, the tubes are externally heated by burning an additional amount of methane and, in some configurations, tail gases. In such conventional reactor configurations, however, the fuel combustion is responsible for roughly 40% of the CO_2 emission of this process [4,6,9]. Moreover, it is estimated that the industrial MSR process accounts for around 3% of global CO_2 emission [10]. Heat transfer limitations of methane steam reforming have been a subject of research for decades [11–13], since the process is mainly limited by the heat fluxes that can be handled without exceeding the maximum operative temperature of the tubes leading to temperature maldistributions inside the reactor tubes. Significant work has been focused on the intensification of the process and on its down-scaling. Two main approaches have been followed in the literature, i.e., the maximization of the heat transfer surface area thanks to micro-channel reactors and the maximization of heat transfer performances thanks to the adoption of conductive internals. As an example, Ashraf and coworkers reported experimental testing of a plate-reactor where combustion is coupled with reforming reactions, enabling a strong process intensification [14]. Due to the complexity of the steam reforming process, Pourali and coworkers systematically worked on modelling parametric analysis to understand the process performance in hydrogen production by steam reforming techniques [15–17]. They suggest that the wall thickness of the microchannel acts as one of the most critical parameters determining the catalytic activity and system efficiency [15]. Another approach was followed by Balzarotti and co-workers [11,12], where the heat transfer in the MSR tubular reactor was improved by the use of conductive internals (*e.g.*, open-cell foams): according to the authors, this solution improved the effective heat conductivity allowing for a three-fold improvement of the performances.

With renewable electricity becoming more accessible, its exploitation to cover the process heat duty represents a promising way to address the challenge of decarbonization [1,18,19]. Electricity can be converted into heat and transferred to thermally driven chemical reactors [20,21]. Several technological options have been proposed exploiting different "power-to-heat" routes [22,23], such as induction heating [24–27], microwave heating [28–32] as well as Joule heating [33–38] (also known as resistive heating or Ohmic heating). Replacing the heat supply in conventional fuel-fired reformers by electrification is regarded as a promising techno-economical solution, also by considering the economically competitive prices for renewable electricity compared with fossil fuels [39,40]. There are several advantages for electrification of MSR process: (i) by replacing the heat suppliers in conventional fuel-fired reformers with electrification, it is possible to completely eliminate the CO_2 emissions from fuel combustion [40–43]; (ii) by removing the firebox, the size of the reformer plant is substantially reduced [41]; (iii) by bringing the heat supply closer to the catalytic sites could significantly reduce the heat transfer limitations, which are the bottleneck of the conventional MSR process, thus leading to the process intensification and the development of compact reformer units [41,44]; (iv) in comparison to other technologies, the theoretical specific power consumption per hydrogen production is estimated at approx. 1.0 kWh/Nm^3_{H2} for electrified MSR [45], which is remarkably less than that of water electrolyzers (3.8–4.5 kWh/Nm^3_{H2}) [45,46].

Different from induction heating or microwave heating, which involve the conversion of electrical energy to electromagnetic energy, Joule heating is in principle the only one that enables the direct transformation of electrical into thermal energy. For this reason, an intrinsically higher thermal efficiency can be expected from Joule heating. Moreover, Joule heating is widely spread in industrial applications, enabling to reach significant temperature and power densities. For this reason, it can be easily integrated in existing plants, enabling a paradigm shift in the design of small-scale reformers. Recently, Wismann and coworkers proposed an innovative reactor concept for direct Joule heating of a Ni-catalyst washcoated FeCrAl-alloy tube for methane steam reforming [41,47,48]. A methane conversion close to 87% was reported with outlet temperatures up to 900°C. By replacing fossil fuel combustion with Joule heating, a CO_2 reduction of 20–50% was achieved when compared with industrial reformers. The authors also reported that the performance of such a configuration with washcoated tubes is mainly controlled by external diffusion, *i.e.*, gas-solid mass transfer, which calls for the adoption of tubes with smaller diameters [47], leading eventually to reactor solutions which are based on either honeycomb monoliths or micro-channel technologies. As an alternative solution, electrical resistances (heating wires) can be inserted into the channels or in the ceramic frame of honeycomb monolith catalysts [49]. Commercial heating elements have been used as catalyst supports: they were activated by washcoating with Ni-based catalysts, and tested in steam and dry reforming [33,34]. These systems are able to reach temperatures in excess of 900°C, and conversions up to 100% as reported by Palma and coworkers [33]. However, the geometry of heating elements is not optimized to be used as a catalyst support, therefore they are associated with both mass transfer limitations and significant bypass that may hinder their applications. Zhang et al. [32] and Zhou et al. [35] studied

plate-type alumina supports impregnated with Ni for electrified methane steam reforming. Zhou et al. [35] reported a high methane conversion of 97% at 700°C, but the employed plate support exhibited a very low hydrothermal stability, *i.e.*, its surface area decreased to only 36% of the initial value after hydrothermal treatment at 700°C for 50 h, which limits its industrialization.

Open-cell foams have been proposed as structured catalyst substrates thanks to their remarkable heat and mass transfer coefficients and large surface areas for catalyst deposition [11–13,50–52]. In this perspective, open-cell foams offer a continuous solid matrix that ensures electrical continuity, which enables distributed heat generation inside the reactor tube and removes the radial heat transfer limitations of conventional reforming [53–55]. For these reasons, a preliminary numerical study was carried out to investigate the electrically heated structured catalysts for the electrified methane steam reforming (eMSR) process [56]. The results suggest that with the right combination of foam geometry, highly active catalyst, and operating conditions, the system can operate in highly intensified conditions.

In our previous work, we have experimentally demonstrated the feasibility of direct Joule heating of SiSiC open-cell foam structures, washcoated with a thin layer of Rh/Al_2O_3 catalyst to perform methane steam reforming [44]. In this work, a systematic study was carried out to further investigate the foam-based eMSR system under a variety of operating conditions in order to better explore the potential of the system and validate a previously developed mathematic model [56]. We have then used the model towards the preliminary scale-up and design of a compact electrified reformer, in view of sustainable H_2 production. In this context, cylindrical Si-infiltrated silicon carbide (SiSiC) foams, washcoated with Rh/Al_2O_3 catalyst with variable catalyst amounts were prepared. The SiSiC foams act not only as catalyst supports but also as the Joule heated resistors, being electrically connected to the power supply. Different operative parameters such as space velocity, operative pressure, steam to carbon ratio and catalyst loadings were investigated to assess their impact on the system performances. The mathematical model previously developed for eMSR systems based on directly heated substrates [56] was able to predict the input-output behavior of the reactor. Intensified experiments and preliminary scale up calculations were carried out aiming at a compact eMSR system for distributed hydrogen production.

Materials and methods

Catalyst preparation and SiSiC foam activation

Commercial Si-infiltrated silicon carbide open-cell foams (Erbicol, CH) with cylindrical geometry (diameter $d_{foam} = 3.2$ cm, length $L_{foam} = 9.9$ cm) were adopted in the present work [57]. As reported previously [44], the adopted foams have a cell diameter (d_{cell}) of 3.32 mm and a strut diameter (d_{strut}) of 0.61 mm, a total porosity estimated by ethanol picnometry of 0.88, and a surface to volume ratio evaluated on the bare geometry (Sv) of 740 m^{-1} [58]. The bulk foam material was characterized by X-ray diffraction: the analysis shows that both Si and SiC phases are present [44]. This limits the possible reactivity between SiC and water during reaction conditions, that can lead to detrimental variation of the electrical resistivity during the tests. Thanks to the interconnected geometry and suitable bulk resistivity of the SiSiC foam, its direct Joule heating up to relevant temperatures for methane steam reforming is feasible [44].

The 1% Rh/Al_2O_3 catalyst powder was prepared by an incipient wetness impregnation method, using γ-Al_2O_3 powder (Sasol, PURALOX) as morphological support and rhodium (III) nitrate solution (Rh 10–15% w/w, Alfa Aesar) as rhodium precursor. The precursor solution was mixed with γ-Al_2O_3 and the obtained powders were dried in oven at 120°C overnight. The detailed catalyst synthesis steps are described in our previous study [44]. In order to catalytically activate the SiSiC foams, a catalyst slurry was prepared. In general, PVA (polyvinyl alcohol, Sigma-Aldrich) was dissolved (0.08:1 w/w with respect to the powder mass) in deionized water (1.8:1 w/w with respect to the powder mass) by magnetic stirring at 85°C. Subsequently, glycerol (Sigma-Aldrich) was added (1.9:1 w/w with respect to the powder mass) and the resulting mixture was stirred until a homogeneous solution was obtained. The solution was then mixed with catalyst powders and ball-milled for 24 h (50 rpm). Afterwards, a small amount of ethanol was added to defoam the slurry.

In order to activate the SiSiC foams for methane steam reforming, the adopted foams were washcoated with a Rh/Al_2O_3 catalyst, which was achieved by dipping the foams in the previously obtained catalyst slurry, followed by spinning (1000 rpm for 10 s) to remove the excess material and by flash drying in oven at 350°C for 5 min [11,44]. Since our experimental setup allows to preheat the water and methane feed at 200°C, only a portion of the foam (4/5 of the total length) was catalytically activated. In this way, the initial bare portion of the foam can be used to heat the gas up to reasonable temperatures to activate the reforming reaction. The coating procedure steps were repeated several times till the desired mass of loaded catalyst was reached. The obtained washcoated foams were then subjected to a conditioning treatment at 500°C for 4 h in flowing N_2. In this work, four washcoated foams were prepared for the purpose of different catalytic tests. The characteristics of the coated foams such as the coated portion of the foam length, the catalyst loading, the coating thickness as well as catalyst density are summarized in Table 1. The coating thickness was calculated by assuming a coating density of 1.3 g/cm^3 [44,59]. Images of the obtained washcoated SiSiC foams and the corresponding catalyst loadings during the multistep coating process are reported in *Supplementary Information, Section S2*.

Catalytic tests

Fig. 1 presents the schematic representation of the electrified methane steam reforming reactor layout, already described in our previous work [44]. In general, the washcoated SiSiC foam was placed in a tubular stainless-steel reactor (OD = 5 cm) for eMSR experiments. A ceramic tube was inserted between the foam and the stainless-steel tube to avoid electric contact. To connect the foam with the DC power generator, home-made electric contactors were adopted, these elements are made

Table 1 – Properties of the four washcoated SiSiC foams investigated in the present work.

Washcoated foams	Coating length [ratio with foam]	Catalyst loading [g]	Coating thickness [μm]	Catalyst density [g/L][a]	Catalytic test
Foam A	4/5	2.2	35.0	34.5	Space velocity effect
Foam B	4/5	2.5	39.8	39.3	Pressure study
Foam C	4/5	2.6	41.4	40.9	Low S/C test
Foam D	4/5	5.5	87.5	86.3	Intensification

[a] Catalyst density referred to the coated zone.

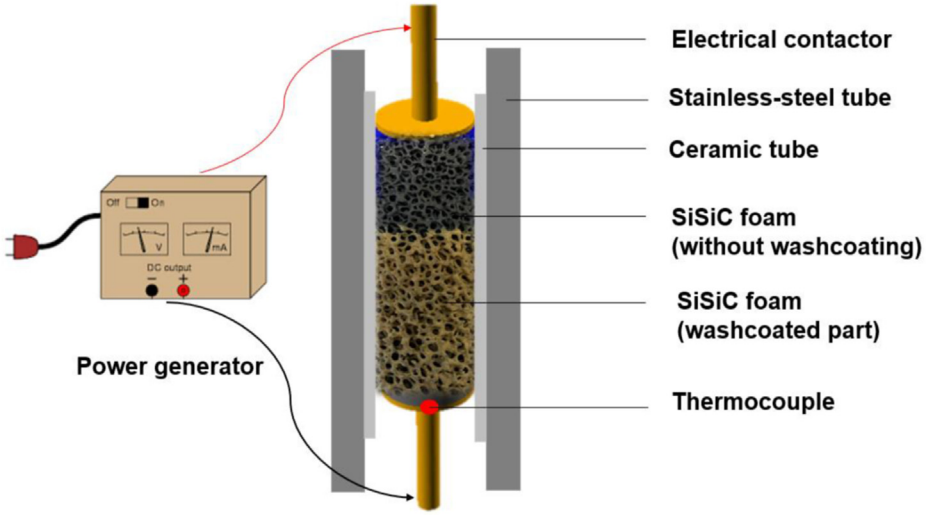

Fig. 1 – Schematic diagram of the electrified methane steam reforming reactor layout. Thermocouple indicates where the T_{down} temperature is measured. The illustration is not to scale.

of stainless-steel cylindrical plates, provided with some holes for gas flow and welded to a ¼' stainless steel pipe. A thin layer of copper foam (Alantum, pore size 800 μm, 1 mm thickness) was placed between the SiSiC foam and the electrical contactor to ensure a good electrical contact. Moreover, an external metallic frame structure built with aluminum bars and threaded rods was adopted to apply additional force to the electrical contactors to counteract their thermal expansion. The contactors are connected to a power generator (STAMOS, S-LS-76, $V_{max} = 30$ V, $I_{max} = 50$ A), which applies a DC current to the system. K-type thermocouples, electrically insulated by ceramic thermowells (dense alumina, $d_{out} = 3$ mm, $d_{in-} = 2$ mm), are placed inside the tube that composes the electric contactors to measure the temperatures at the top and bottom of the foam.

The gases were fed to the system individually by means of mass flow controllers (Brooks 5851), while water was fed with a dosing-evaporation system (Brooks, Quantim QMBC3L). In a typical experiment, the system was pre-heated in nitrogen above 500°C, then water was fed to the system; afterwards, the flow of nitrogen was switched to methane to start the MSR reaction. Catalytic tests were performed with a non-diluted gas feed of CH_4 and H_2O, with steam to carbon ratio (S/C) of 3 and 4.1, at gas hourly space velocity (GHSV) in the range of 50000–200000 Nl/h/kg_{cat}, and different operating pressures ranging from 1 to 3 bar. For each test, the target downstream temperature (T_{down}, as shown in Fig. 1) was achieved by adjusting the input electric voltage. The current output is a self-adjusted parameter of the circuit, and its measurement enables the calculation of the input power and of the overall resistance of the system, including possible contact/wiring resistances. Downstream the reactor, water was removed from the products by a condenser working at 2°C and the dry gas mixture was analyzed using an online micro-GC (Agilent, 900 Micro GC). To enable the use of internal standard, an inert gas (nitrogen) was directly fed to the analysis section through a by-pass line. Optimal analytical conditions were obtained by setting the nitrogen flowrate at 1/3 of the inlet methane flowrate. For each catalytic test, the catalytic performance, the electrical behavior as well as the thermal efficiency of the system were evaluated; the detailed data analysis methods are described in *Supplementary Information, Section S1*. The carbon balance was monitored and was very close to 100% of the converted carbon during all the eMSR tests.

Mathematical model

The experiments described above were used to validate a mathematical model of the Joule-heated foam-based unit, that was developed in our previous work [56]. Details of model assumptions and equations and of the numerical solution methods are reported in *Supplementary Information (Section S3)*.

The concept mathematically described by the model equations is that a perfectly mixed stream of CH_4 and water is

fed to a cylindrical reactor wherein it contacts a catalytically active and electrically heated solid phase The solid pseudo-phase accounts for SiSiC foam, coated with a thin catalyst layer where endothermic steam reforming occurs. Since the catalyst is in intimate contact with the support, any heat transfer resistance between the solid phases can be neglected, convective mechanisms governing the energy and mass transfer between the flowing gaseous mixture and the solid pseudo-phase.

A 2D heterogeneous reactor model was adopted to calculate both axial and radial distributions of temperature/concentrations in the gas and the solid phase in the presence of heat losses. For this purpose, both mass and energy balances (including the Joule heating generation term) were solved, alongside with the momentum balance to account for the pressure drop. To account for transport properties in open-cell foams, correlations previously developed in our group have been adopted [50,51,60]. A kinetic scheme including methane steam reforming and the water gas shift reaction was implemented with rate expressions adapted from our previous kinetic study of methane steam reforming over the same Rh-based catalyst in concentrated conditions [13]. In the original study, intrinsic kinetic parameters were referred to the egg-shell volume of spherical pellets; since the same carrier, active phase and Rh content of the active shell layer was herein replicated in the form of foam-washcoat, the same intrinsic parameters were incorporated. Diagnostic calculations based on the estimation of effectiveness factors ruled out significant internal mass transfer limitations.

Heat losses in the thermal insulation were calculated consistently with the description provided in our previous work [56], considering in series the thermal resistance provided by the thermal insulation layer and the superficial heat transfer coefficient of the reactor in ambient air. The resulting sets of PDEs was discretized by centered finite differences in the axial direction and symmetric orthogonal collocations in the radial direction. A grid of equi-spaced 81 axial points and 4 radial points assigned in the roots of the Jacobi polynomials was considered. Matlab solver *fsolve* with sparse Jacobian pattern was then used to solve the resulting algebraic system.

Results and discussion

Effect of space velocity

Methane steam reforming tests were run at various T_{down} temperatures by controlling the input power, which was achieved by adjusting the input voltage. Fig. 2(a) shows the outcome of the measured T_{down} temperature with the input power at different space velocities during eMSR based on Foam A (*c.f.* Table 1 and Fig. S1). T_{down} temperature exhibited an almost linear correlation with the input power, which is consistent with our previous results [44]. As expected, more input power was required with increasing space velocities. For example, a high input power of 584 W was required to reach a T_{down} temperature of 750°C at 200000 Nl/h/kg_{cat}, whereas only 314 W was necessary to reach the same temperature at 50000 Nl/h/kg_{cat}. For a given space velocity, upon increasing the input power, the methane conversion grew progressively (Fig. 2(b)), and full methane conversion was achieved for all the investigated GHSV values. For the space velocity of 50 000 Nl/h/kg_{cat}, full methane conversion was achieved with an input power of 216 W and at a T_{down} temperature of 650°C, while at a space velocity of 200000 Nl/h/kg_{cat} a power of 584 W and a T_{down} temperature of 700°C were needed to reach the same conversion.

The measured methane conversion is also plotted as a function of T_{down} temperature in Fig. 3(a). In general, full conversion was achieved above 700°C for all the investigated space velocities. It is noted that the experimental conversions moderately exceeded the equilibrium conversions at low space velocities; this reveals that the measurement of T_{down} temperature is to some extent lower than the actual outlet temperature of the foam, that is not in direct contact with the electrified support and is inserted in a thermowell made of an electrically and thermally insulating material (Fig. 3(b)). It should be mentioned that it is challenging to measure the actual temperature inside the foam due to electric concerns: this is a common problem in electricity driven reactors [29,61,62].

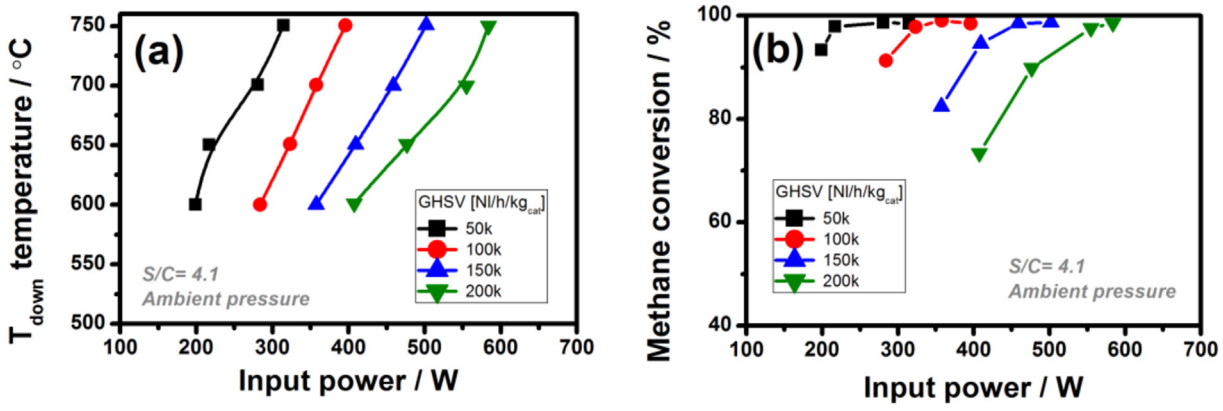

Fig. 2 – (a) T_{down} temperature and (b) methane conversion as a function of input power during electrified methane steam reforming at different space velocities. Experimental conditions: Foam A, 1% Rh/Al_2O_3 washcoated (4/5) on SiSiC foam with a catalyst loading of 2.2 g, feed mixture of CH_4 and H_2O with steam to carbon ratio (S/C) of 4.1, gas hourly space velocity (GHSV) of 50000 Nl/h/kg_{cat}, 100000 Nl/h/kg_{cat}, 150000 Nl/h/kg_{cat} and 200000 Nl/h/kg_{cat}, ambient pressure.

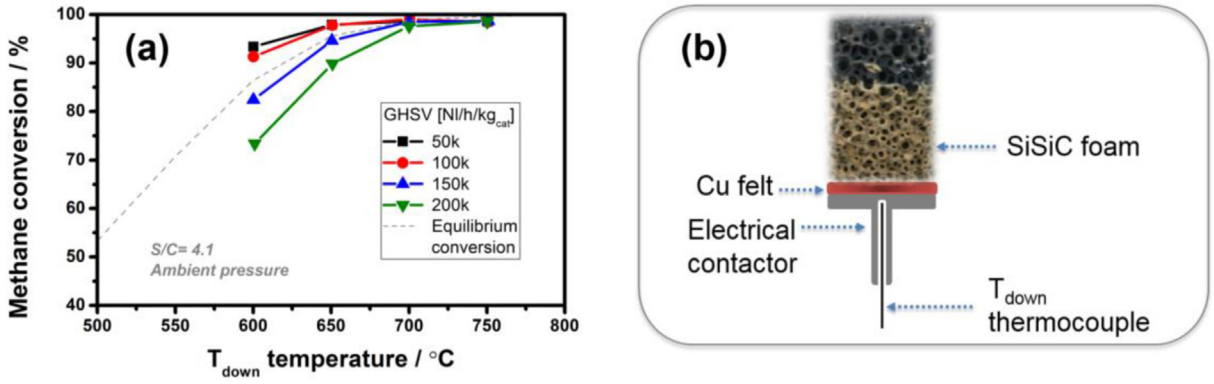

Fig. 3 – (a) Methane conversion as a function of T_{down} temperature during electrified methane steam reforming at different space velocities. (b) Schematic representation of the T_{down} temperature measurement during proposed electrified methane steam reforming system. Experimental conditions: Foam A, 1% Rh/Al_2O_3 washcoated (4/5) on SiSiC foam with a catalyst loading of 2.2 g, feed mixture of CH_4 and H_2O with steam to carbon ratio (S/C) of 4.1, ambient pressure and gas hourly space velocity (GHSV) of 50000 Nl/h/kg_{cat}, 100000 Nl/h/kg_{cat}, 150000 Nl/h/kg_{cat} and 200000 Nl/h/kg_{cat}, ambient pressure.

The electric behavior of the foam-based eMSR system was also evaluated and the results are presented in Fig. 4(a). Upon increasing the input power, both the input voltage and the current increas about linearly within the investigated conditions (Fig. 4(a)). An electrical resistance in the range of 0.42–0.62 Ω was estimated based on the input voltage to current ratio (Table S1). The electrical resistance slightly decreased with increasing temperature, in line with the positive effect of temperature on the electrical resistance of SiC heating elements reported by Pelissier and cowokers [63], as well as our previous results [44]. The effective resistivity of the foam was estimated in the range of 3.4–5 × 10^{-3} Ω m, which according to (Eq. S5) corresponds to an intrinsic resistivity of the SiSiC material in the range of 1.5–2.2 × 10^{-4} Ω m, in line with the values reported for commercial SiC elements in the investigated temperature region [63]. Some small oscillations may be due to the onset of contact resistances.

In designing the heating elements, it is also important to remind that all materials are characterized by a maximum dielectric voltage – higher values may lead to spontaneous electric discharges in the material. The maximum current density that can be carried by the element should be carefully checked when designing such systems.

Fig. 4(b) shows values of electric field (V/m) and current density (A/m^2) as a function of power density (MW/m^3). It is possible to note that the investigated system operates with input power densities in the range of 2.5–7.4 MW/m^3. This is comparable to conventional industrial scale fired reformer tubes, which are typically operated up to 7.5 MW/m^3 [64]. Electric field and current densities are of great interest for tentative sizing of scaled-up units with the same foams (material, porosity). They both increase approximately linearly with power density. The highest electric field of 163.2 V/m and the highest current density of about 45000 A/m^2 were achieved with the power density of 7.4 MW/m^3.

Fig. 5 (a) shows the H_2 productivity as a function of T_{down} temperature taken from eMSR tests performed at various operating space velocities. The H_2 productivity was calculated based on the measured H_2 yield and considering a WGS unit operating at T = 200°C downstream the eMSR to increase the

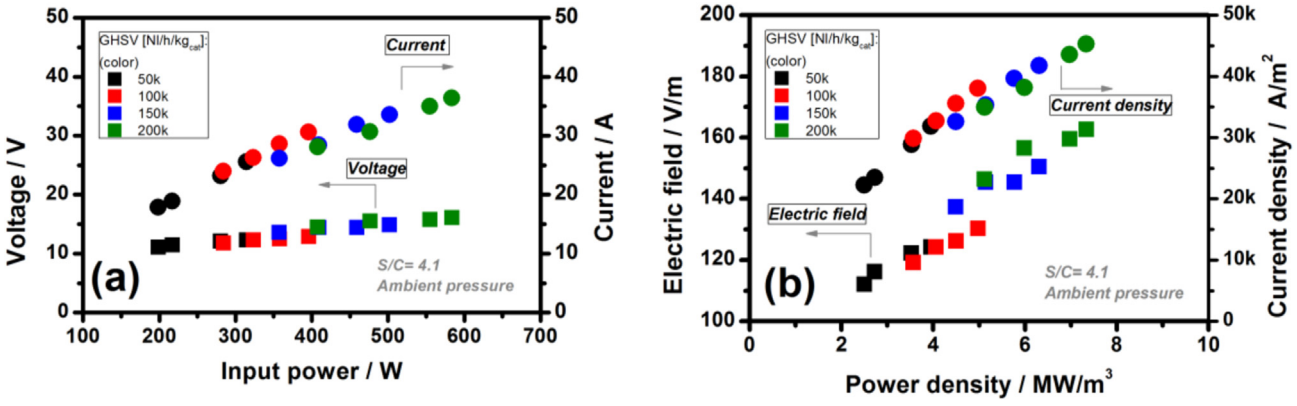

Fig. 4 – (a) Input voltage and current as a function of input power and (b) electric field and current density as a function of power density during electrified methane steam reforming. Experimental conditions: Foam A, 1% Rh/Al_2O_3 washcoated (4/5) on SiSiC foam with a catalyst loading of 2.2 g, feed mixture of CH_4 and H_2O with steam to carbon ratio (S/C) of 4.1, gas hourly space velocity (GHSV) of 50000 Nl/h/kg_{cat}, 100000 Nl/h/kg_{cat}, 150000 Nl/h/kg_{cat} and 200000 Nl/h/kg_{cat}, ambient pressure.

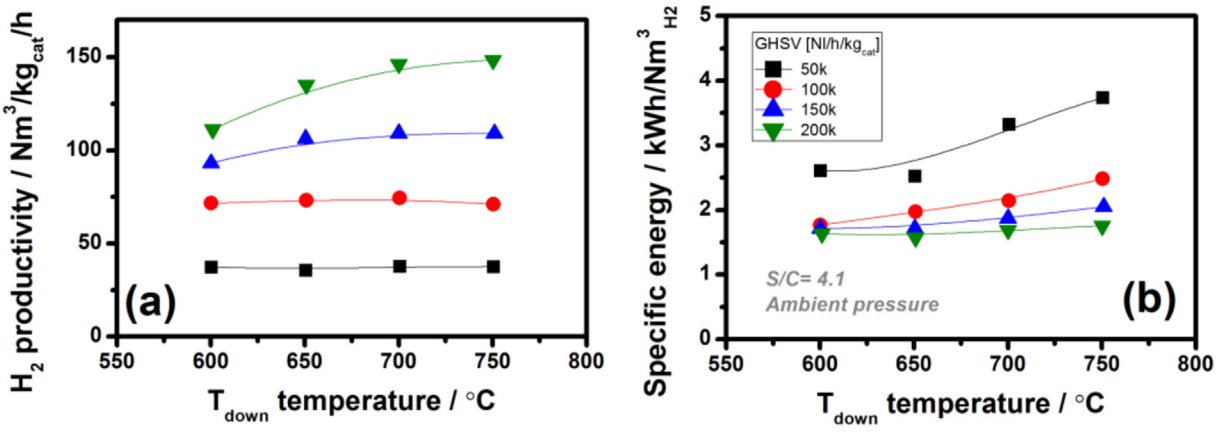

Fig. 5 – (a) Hydrogen productivity and (b) specific energy demand for hydrogen production as a function of T_{down} temperature during electrified methane steam reforming runs at different space velocities. Hydrogen yield is calculated considering complete water-gas shift reaction, i.e. assuming that CO is fully converted to CO_2. Experimental conditions: Foam A, 1% Rh/Al_2O_3 washcoated (4/5) on SiSiC foam with a catalyst loading of 2.2 g, feed mixture of CH_4 and H_2O with steam to carbon ratio (S/C) of 4.1, gas hourly space velocity (GHSV) of 50000 Nl/h/kg_{cat}, 100000 Nl/h/kg_{cat}, 150000 Nl/h/kg_{cat} and 200000 Nl/h/kg_{cat}, ambient pressure.

H_2 productivity and convert almost completely CO to CO_2, which can be easily separated from the gaseous stream. The corresponding results for hydrogen productivity and specific energy for hydrogen production considering the composition measured at the out of the reactor are presented in Fig. S5.

The obtained results show that hydrogen productivity increased almost linearly with the space velocity, since the system was operated close to thermodynamic equilibrium. The foam-based eMSR system achieved a hydrogen productivity over 150000 Nl/kg_{cat}/h, which is much higher than that of conventional steam reformers [4]. However, it worth to note that this system uses a washcoated Rh catalyst, which allows a much higher effectiveness factor than conventional pellet catalysts. Fig. 5 (b) shows the specific energy for hydrogen production as a function of T_{down} temperature. The specific energy consumption decreased with increasing space velocity. The lowest value of 1.57 kWh/Nm^3_{H2} was achieved at GHSV = 200000 Nl/h/kg_{cat}. This is significantly lower compared to the values reported for water electrolyzers (3.8–4.5 kWh/Nm^3_{H2}) [45,46].

The energy efficiency (η) of the system, defined as the ratio between the enthalpy gain Q (Eq. (3)) and the electric power input P, is thus limited by the power losses (P_{loss}) of the system (Eq.s 4 and 5), and is plotted against T_{down} in Fig. 6(a).

$$Q = \dot{H}_{out} - \dot{H}_{in} \tag{3}$$

$$P_{loss} = P - Q \tag{4}$$

$$\eta = Q/P = 1 - P_{loss}/Q \tag{5}$$

where $\dot{H}_{in}$ and $\dot{H}_{out}$ are the enthalpy flows of the gas mixtures at inlet and outlet of the reactor, respectively.

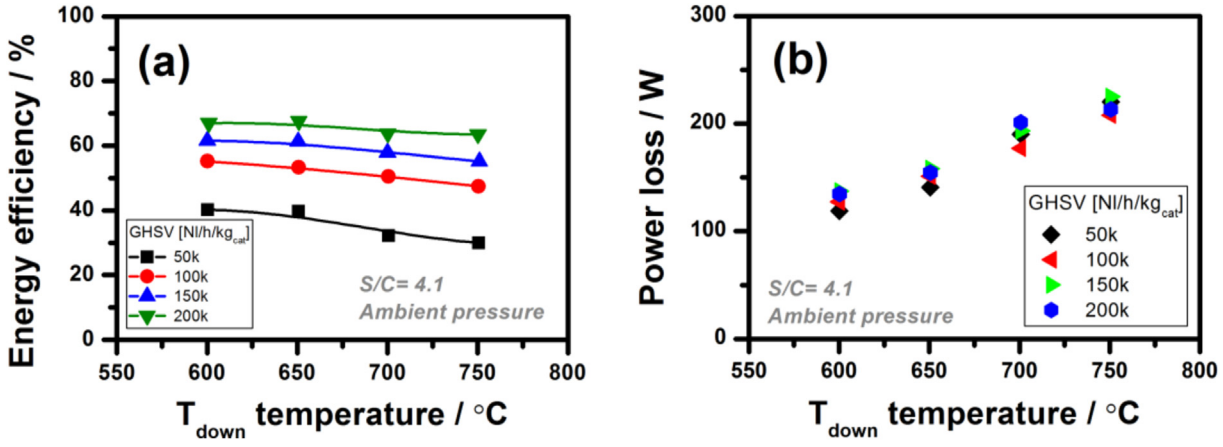

Fig. 6 – (a) Energy efficiency and (b) power loss as a function of T_{down} temperature during electrified methane steam reforming at different space velocities. Experimental conditions: Foam A, 1% Rh/Al_2O_3 washcoated (4/5) on SiSiC foam with a catalyst loading of 2.2 g, feed mixture of CH_4 and H_2O with steam to carbon ratio (S/C) of 4.1, gas hourly space velocity (GHSV) of 50000 Nl/h/kg_{cat}, 100000 Nl/h/kg_{cat}, 150000 Nl/h/kg_{cat} and 200000 Nl/h/kg_{cat}, ambient pressure.

The energy efficiency markedly increased with increasing space velocity, i.e. with the inlet flow rate, achieving the highest value of approx. 70% at GHSV = 200000 Nl/h/kg_{cat}. This is due to the fact that the input power markedly increased with GHSV (Fig. 2), while, as illustrated in Fig. 6(b) and in line with our previous results [44], power losses, (Eq. (5)), instead grew almost linearly with the reactor temperature and were independent of the space velocity. This indicates that heat dissipation out of the reactor walls in eMSR was mainly responsible for energy losses. In fact, the ohmic losses in the wiring are linear with the input power and were estimated to be approx only 3% of the total loss [56].

Overall, the enthalpy gain increased with increasing space velocity, while the heat dissipation practically kept the same at a given reactor temperature. Therefore, the energy efficiency grew with the operating space velocity, resulting in lower values of the specific energy consumption. This indicates that much higher efficiency could be achieved by scaling up the system, as investigated by mathematical modelling in the following Section on Scale-up considerations.

Effect of pressure

The operating pressure is one of the crucial parameters for methane steam reforming. The global reaction is characterized by an increasing number of moles, therefore, equilibrium conversion decreases with increasing operative pressure, according to the Le Chatelier principle [65,66]. Kinetics of MSR over Rh catalyst are instead considered to be pseudo first-order, therefore they are beneficially affected by the pressure. Industrial MSR processes typically operate at pressures up to 30 bar, and this requires temperatures higher than 900°C to achieve high CH_4 conversion [67]. Such a choice is justified by economic reasons [68,69]. In fact, by operating under pressure, the productivity per volume of the reactor increases, furthermore less energy for compression is required if the final H_2 is utilized for high pressure applications, such as ammonia synthesis [67,68]. Pressure for small scale steam reforming applications, *e.g.* biogas reforming, H_2 production for combined heat and power (CHP) applications, is typically lower, from atmospheric to 8–10 bar [70]. The tradeoff between equipment cost, operative temperature (material cost) and H_2 separation technology drives the choice of operating in these conditions. The effect of pressure on the thermodynamic H_2 cold gas efficiency has been reported in our previous work [56], showing that operating at lower pressure maximizes H_2 yield and the energy effectively conveyed in it at fixed temperature.

Another catalyst washcoated SiSiC foam, *i.e.* Foam B, was prepared to study the pressure effect on the foam-based eMSR system. Similar to Foam A, 4/5 of Foam B was washcoated with a catalyst loading of 2.5 g (Fig. S2). This corresponds to a catalyst thickness of 39.8 μm and a coating density of 39.3 g/L (Table 1).

The pressure study was carried out at two space velocities of 100000 Nl/h/kg_{cat} and 200000 Nl/h/kg_{cat}, for each feed condition the operating pressures of 1 bar, 2 bar and 3 bar were investigated at T_{down} temperature of 650 °C and 700 °C. Fig. 7 shows the measured methane conversion as a function of T_{down} temperature. At ambient pressure with GHSV of 100000 Nl/h/kg_{cat}, methane conversions of 96% and 98.5% were achieved at a T_{down} temperature of 650°C and 700°C, respectively (Fig. 7(a)). These values are comparable to those obtained on Foam A in the corresponding conditions, indicating a good reproducibility of the experiments. Operating the system at higher pressures leads to a progressive decrease in methane conversion, with only 88% and 95% observed at 3 bar for 650°C and 700°C, respectively. A similar trend was noticed as well for high space velocity conditions (GHSV = 200000 Nl/h/kg_{cat}, Fig. 7(b)). These results show a systematic negative effect of the pressure on the methane conversion for all the conditions. The methane conversions were also compared to the thermodynamic equilibrium conversions and the results are shown in Fig. S6. A slight overshoot of the experimental results beyond the equilibrium conversion was noticed,

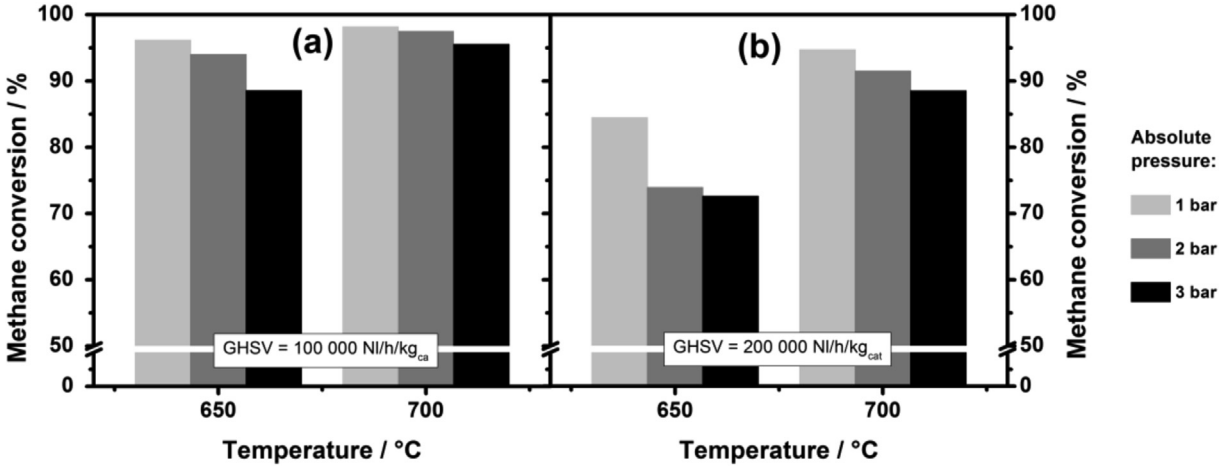

Fig. 7 – Comparison of methane conversion during pressure experiments at T_{down} temperature of 650°C and 700°C: (a) GHSV = 100000 Nl/h/kg_{cat} and (b) GHSV = 200000 Nl/h/kg_{cat}. Experimental conditions: Foam B, 1% Rh/Al_2O_3 washcoated (4/5) on SiSiC foam with a catalyst loading of 2.5 g, feed mixture of CH_4 and H_2O with steam to carbon ratio (S/C) of 4.1, gas hourly space velocity (GHSV) of 100000 Nl/h/kg_{cat} and 200000 Nl/h/kg_{cat}, operating pressure of 1 bar, 2 bar and 3 bar.

especially at high operating pressures, for the reasons explained previously. In addition, the corresponding electric behavior of Foam B was evaluated and the results are shown in Table S2.

Fig. 8 shows the H_2/CO ratio obtained from the pressure experiments, which is in the range of 7.5–10.3 in the investigated conditions. It can be observed that with the increase of operating pressure, the syngas produced was characterized by a higher fraction of hydrogen compared to carbon monoxide. Such a trend was observed at both levels of temperature and space velocity. This could be explained by the fact that lower methane conversions under pressure conditions result in higher outlet water concentrations which push WGS equilibrium towards H_2 formation [13]. Such an explanation could be further supported by the decrease of CO/CO_2 ratios at high operating pressures (Table S2).

Fig. 9 presents the hydrogen productivity and specific energy consumption during the pressure effect experiments. The values at ambient pressure are consistent with previous results on Foam A, including the trend of the temperature and space velocity effect. A hydrogen productivity of approximately 150 $Nm^3/h/kg_{cat}$, accompanied by a very low specific energy consumption of 1.6 kWh/Nm^3_{H2}, was achieved with GHSV of 200000 $Nl/h/kg_{cat}$, T_{down} of 700°C under ambient pressure.

As a result of the negative effect of pressure on conversion (Fig. 7), the hydrogen productivity decreased when passing from 1 to 3 bar, as shown in Fig. 9(a). At GHSV of 200000 $Nl/h/kg_{cat}$ and T_{down} of 700°C, hydrogen productivity of 141 $Nm^3/kg_{cat}/h$ and 134 $Nm^3/kg_{cat}/h$ was obtained for operating pressure of 2 bar and 3 bar, respectively. The same pressure effect was noticed under GHSV of 100000 $Nl/h/kg_{cat}$, however the negative effect of pressure is less evident than at the higher space velocity.

The specific energy consumption (Fig. 9(b)) was negatively affected by the operating pressure, as 1.67 kWh/Nm^3_{H2} and 1.71 kWh/Nm^3_{H2} were needed at 2 bar and 3 bar, respectively, at GHSV of 200000 $Nl/h/kg_{cat}$ and T_{down} of 700°C. The corresponding results of hydrogen productivity and specific energy

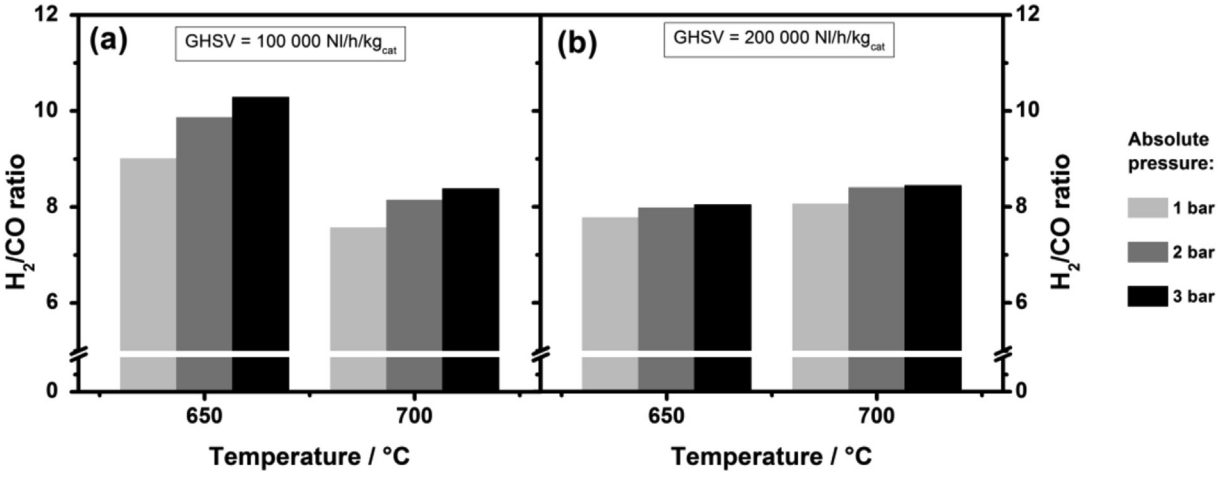

Fig. 8 – H_2/CO ratios during pressure experiments at T_{down} temperature of 650°C and 700°C: (a) GHSV = 100000 $Nl/h/kg_{cat}$ and (b) GHSV = 200000 $Nl/h/kg_{cat}$. Experimental conditions: Foam B, 1% Rh/Al_2O_3 washcoated (4/5) on SiSiC foam with a catalyst loading of 2.5 g, feed mixture of CH_4 and H_2O with steam to carbon ratio (S/C) of 4.1, gas hourly space velocity (GHSV) of 100000 $Nl/h/kg_{cat}$ and 200000 $Nl/h/kg_{cat}$, operating pressure of 1 bar, 2 bar and 3 bar.

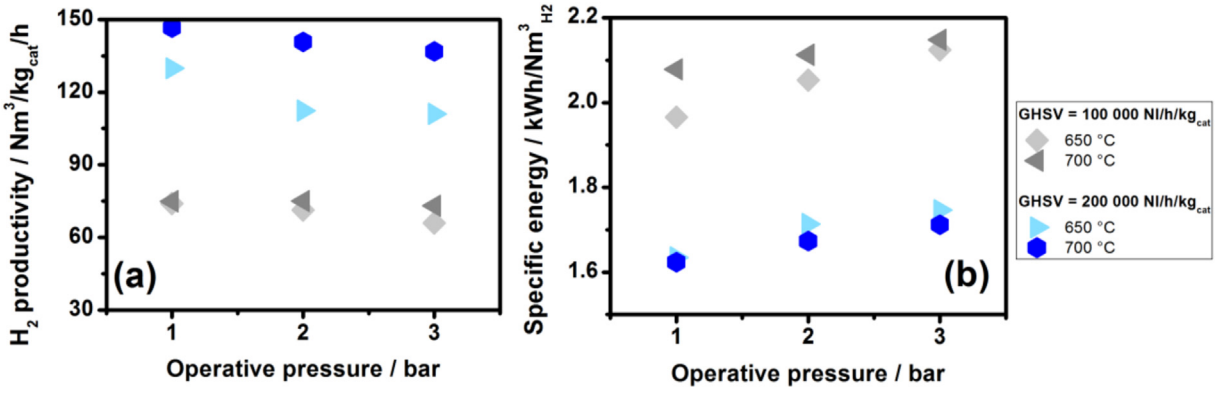

Fig. 9 – (a) Hydrogen productivity and (b) specific energy for hydrogen production as a function of operative pressure during electrified methane steam reforming. Hydrogen yield is calculated considering complete WGS reaction, i.e. assuming that CO is fully converted to CO_2. Experimental conditions: Foam B, 1% Rh/Al_2O_3 washcoated (4/5) on SiSiC foam with a catalyst loading of 2.5 g, feed mixture of CH_4 and H_2O with steam to carbon ratio (S/C) of 4.1, gas hourly space velocity (GHSV) of 100000 $Nl/h/kg_{cat}$ and 200000 $Nl/h/kg_{cat}$, operating pressure of 1 bar, 2 bar and 3 bar.

consumption without considering the downstream water-gas shift reaction are presented in Fig. S7. The overall energy efficiency of the system was observed to decrease with increasing operating pressure, as shown in Fig. S8.

The obtained results show the potential of the proposed foam-based eMSR system to operate under mild pressure conditions. This offers promising flexibility of the system to be integrated with downstream applications where operating under pressure is required [67,68]. Moreover, the pressurized operation of the reactor is of potential interest for the integration of eMSR with membranes for the production of high purity H_2 [71–73], such as Pd-based membranes [74,75].

Tests at lower S/C ratio

The catalytic performance of the proposed foam-based eMSR system with steam to carbon feed ratio of 3 was evaluated over Foam C (4/5 washcoated foam with catalyst loading of 2.6 g, *c.f.* Fig. S3). The catalytic test was carried out at GHVS = 150000 Nl/h/kg_{cat}, and ambient pressure, and the results are shown in Fig. 10. Almost full methane conversion was obtained at T_{down} of 750°C, however conversions lower than equilibrium were observed at lower temperatures, indicating that the process is kinetically controlled in such conditions, due to the higher amount of methane moles in the feed. The results are in line with previous results obtained on Foam A under the same space velocity but a higher steam to carbon ratio of 4.1(Fig. 10). Moreover, it is obvious that a lower S/C ratio resulted in lower methane conversions at the same reactor temperature. This is consistent with the thermodynamic constraints of the process and in line with literature reports [76]. Even with lower methane conversions, the low S/C operation (Table 2) shows similar energy efficiency and specific energy for hydrogen production in comparison to S/C of 4.1 (Figs. 6(a) and Fig. 5(b)). However, higher hydrogen productivities were observed for S/C = 3, which can be explained by the higher CH_4 concentration in the gas feed. In general, the reforming catalysts exhibit a higher coking tendency at low steam to carbon ratios [77], but S/C of 3 should be a safe condition, especially for highly active Rh-based catalysts [78]. It should be mentioned that the system is stable under such low steam to carbon ratio conditions. For each temperature, the system was kept at a steady state for at least 20 min, without observing any loss of catalytic activity.

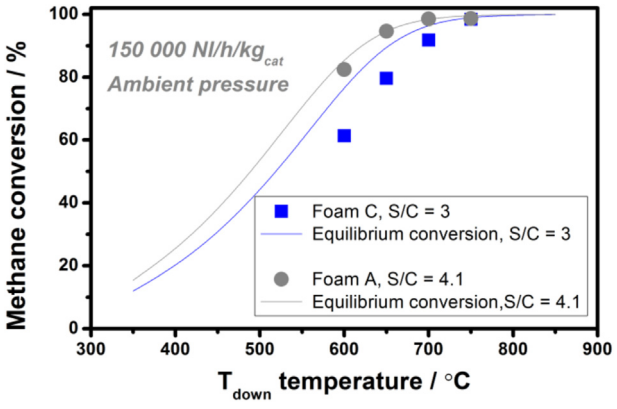

Fig. 10 – Methane conversion as a function of T_{down} temperature during electrified methane steam reforming at different S/C ratios. Experimental conditions: gas hourly space velocity (GHSV) of 150000 Nl/h/kg_{cat}, ambient pressure; Foam C, 1% Rh/Al_2O_3 washcoated (4/5) on SiSiC foam with a catalyst loading of 2.6 g, feed mixture of CH_4 and H_2O with steam to carbon ratio (S/C) of 3; Foam A, 1% Rh/Al_2O_3 washcoated (4/5) on SiSiC foam with a catalyst loading of 2.2 g, feed mixture of CH_4 and H_2O with steam to carbon ratio (S/C) of 4.1.

Tests with higher catalyst loading

In order to further exploit the potential of the foam-based eMSR system to operate in intensified conditions, Foam D was prepared with a higher catalyst density and studied. As summarized in Table 3, the catalyst loading of 5.5 g was achieved after 11 coating cycles (Fig. S4). This corresponds to a catalyst density of 86.3 g/L and a washcoat thickness of about 87.5 μm. After loading the washcoated foam to the reactor, the same conditioning treatment and testing strategies were performed as previously introduced.

Fig. 11 exhibits the measured methane conversion as a function of T_{down} temperature on Foam D during catalytic tests with space velocity of 150000 Nl/h/kg_{cat}, ambient pressure. The measured methane conversions were less than the thermodynamic equilibrium conversions at 600°C and 650°C. Slightly lower conversions compared to those obtained on Foam A were noticed in corresponding conditions (Fig. 3). Nevertheless, almost full conversions were achieved at 700°C–750°C for the investigated space velocity (Fig. 11). As a result of high conversion, a high hydrogen productivity of 118 $Nm^3/kg_{cat}/h$ and the lowest specific energy consumption of only 1.24 kWh/Nm^3_{H2} were achieved (Table 3). In this regard, the obtained results verified the excellent ability of the proposed foam-based eMSR system for hydrogen production in

Table 2 – Summary of the experimental results obtained from Foam C. The specific energy consumption (e^*) for hydrogen production and the hydrogen productivity (P^*_{H2}) were calculated considering a downstream complete water gas shift reaction assuming that CO is fully converted in to CO_2. Foam C: 4/5 coating length, 2.6 g catalyst loading, 41.4 μm; 40.9 g/L. Experimental conditions: S/C = 3; GHSV = 150000 Nl/h/kg_{cat}, ambient pressure.

T_{down} [°C]	Voltage [V]	Current [A]	Resistance [ohm]	X_{CH4} [%]	e^* [kWh/Nm^3_{H2}]	P^*_{H2} [$Nm^3/kg_{cat}/h$]	Energy efficiency η [%]
750	16.8	39.2	0.43	98.4	1.91	136	58
700	16.3	36.6	0.45	91.7	1.84	128	57
650	15.4	33.0	0.47	79.6	2.03	99	57
600	13.9	28.0	0.50	61.3	2.24	68	57

Table 3 – Summary of the experimental results collected on Foam D. The specific energy consumption (e^*) for hydrogen production and the hydrogen productivity (P^*_{H2}) were calculated considering a downstream complete water gas shift reaction assuming that CO is fully converted into CO_2. Foam C: 4/5 coating length, 5.5 g catalyst loading, 87.5 μm; 86.3 g/L. Experimental conditions: S/C = 4.1; GHSV = 150000 Nl/h/kg_{cat}, ambient pressure.

T_{down} [°C]	Voltage [V]	Current [A]	Resistance [ohm]	X_{CH4} [%]	e^* [kWh/Nm^3_{H2}]	P^*_{H2} [$Nm^3/kg_{cat}/h$]	Energy efficiency η [%]
750	18.4	46.4	0.40	98.9	1.32	118	79
700	18.2	43.7	0.42	96.1	1.27	114	79
650	17.5	40.4	0.43	86.2	1.24	104	81
600	16.3	35.5	0.45	64.4	1.34	78	79

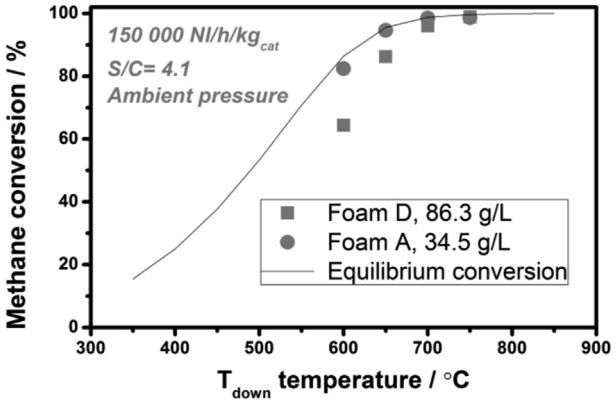

Fig. 11 – Methane conversion as a function of T_{down} temperature during intensified electrified methane steam reforming runs. Experimental conditions: feed mixture of CH_4 and H_2O with steam to carbon ratio (S/C) of 4.1, gas hourly space velocity (GHSV) of 150000 Nl/h/kg_{cat}, ambient pressure; Foam D, 1% Rh/Al_2O_3 washcoated (4/5) on SiSiC foam with a catalyst loading of 5.5 g; Foam A, 1% Rh/Al_2O_3 washcoated (4/5) on SiSiC foam with a catalyst loading of 2.2 g.

intensified condition, *i.e.*, high catalyst inventory with a catalyst density of approx. 86 g/L. Moreover, as a result of a more intensified operation, an energy efficiency of 81% was achieved in the present work, as shown in Table 3. This is quite remarkable considering the relatively small size of the test unit adopted here. It should be noted that further improvement of the energy efficiency is practically feasible, *e.g.*: (i) by further increasing the operating space velocity, (ii) by decreasing the steam to carbon ratio, or (iii) by minimizing the heat dissipation, *i.e.*, exploitation of systems with better thermal insulation and with different geometry. In general, the share of the heat dissipation decreases with scaling up the reactor diameter [56]. This latter point was investigated by mathematical model simulations, as reported below in the *Section* Scale-up considerations.

As discussed in the Introduction section, the electrification of thermally driven catalytic processes could be achieved by induction heating, microwave heating and Joule heating. Table 4 summarizes and compares the recent developments of the eMSR process in terms of different heating methods and reactor configurations. In general, all the electrification methods enable promising methane conversions as a result of enhanced heat transfer. However, on the other hand, induction heated eMSR processes show limited energy efficiencies [79], with the highest value of 23% reported by Almind and coworkers [24]. Meloni et al. [28] reported an energy efficiency of 55% using microwave heating, while a higher value of 73% was achieved by recovering part of the heat dissipation to pre-heat the feed gas [80]. Different from those two heating methods, Joule heating is in principle the only one that enables the direct complete transformation of electricity into thermal energy. As expected, an unprecedented high energy efficiency of 81% was achieved in this work on the washcoated SiSiC foam with a catalyst density of 86.3 g/L (GHSV = 150000 Nl/h/kg_{cat}, S/C = 4.1, ambient pressure), accompanied by a specific energy demand of 1.24 kWh/Nm^3_{H2}, which is remarkably less than that of electrolyzers (3.8–4.5 kWh/Nm^3_{H2}) [45,46]. Those results are superior to our previous work [44], thanks to the more intensified conditions, i.e., higher catalyst density and feed flow rate.

Validation of the mathematical model

As described in equation S34 of Supplementary Information, section S3, a uniform current density was assumed in the whole foam domain to simulate the electric heating of the eMSR reactor. In fact, the resistivity of the SiSiC foam varies with temperature and this would lead in principle to a complex description of the radial variation of the electric field; however, radial temperature gradients in this system were very limited, so the resistivity was considered constant on the radial cross section of the foam and estimated at the radially averaged solid temperature. Experimental tests showed modest test-by-test variations of the overall electrical resistance that cannot be explained by different temperature fields but are due most likely to different electrical contact resistances in the experiments. Therefore, if the experimental current is used, this may lead to spurious changes in the total power supplied to the reactor. To enable a correct simulation of the experimental tests, the current measured in the experiments was adjusted to ensure that the total enthalpy gain (Eq. (3)) in the reactor was equal to the value calculated from the experimental data. The resulting changes of voltages and currents were limited, being in the ±10% range with respect to experimental values.

As an example of the model simulations, the axial temperature profiles and the compositions of the test with set T_{down} equal to 750°C are shown in Fig. S9 of the Supplementary Information. Panel A clearly explains the role of the preheating zone in the design of the lab-scale system. In fact, the solid temperature at the inlet of the catalytic region allows

Table 4 – Summary of recent developments for the electrification of methane steam reforming in terms of different heating strategies, including induction heating, microwave heating and Joule heating.

Heating method	Nr.	Reactor configuration	Experimental conditions	Performances	Ref.
Induction heating	1	Stainless-steel reactor (induction heating susceptor); $Na_{0.5}La_{0.5}Ni_{0.3}Al_{0.7}O_{2.5}$ catalyst; Cu coil.	CH_4/H_2O/inert = 10.5/8.5/1; GHSV = 30000 Nl/kg_{cat}/h.	Full CH_4 conversion at 853°C.	[79]
	2	Quartz tube reactor; Ni–Co based catalysts (also as susceptor); Cu coils.	S/C = 2; GHSV = 8182 Nl/kg_{cat}/h.	X_{CH4} > 90% at 800°C; Energy efficiency of 23%.	[24,81,82]
	3	High temperature tube reactor consists two parts: a reaction cavity inside and around which is a heat transfer cavity: filled with wick structure and sodium as the heat transfer medium.	13.5% Ni/Al_2O_3 catalyst; S/C = 3; GHSV = 37000 h^{-1}; Ambient pressure.	X_{CH4} = ~90% at 650°C.	[25]
Microwave heating	1	Stainless-steel tube reactor with transparent window; Catalyst coated SiC monolith (as susceptor); Ni-based catalysts; Gas flows from up to bottom of the reactor.	S/C = 3; GHSV = 3300 $h^{-1.}$	Equilibrium conversion above 800°C; Energy efficiency of 55%; Energy consumption: 3.8 kW/Nm^3_{H2}.	[28]
	2	Similar reactor with ref. [28], with modified gas path (enters from the top and passes through the inner interspace before entering in the reactor from the bottom).	S/C = 3; GHSV = 5000 $h^{-1.}$	Equilibrium conversion above 750°C; Energy efficiency of 73%; Energy consumption: 2.5 kW/Nm^3_{H2}.	[80]
Joule heating	1	FeCrAl-alloy tube (Joule heating substrate) washcoated with Ni-based catalyst.	$CH_4/H_2O/H_2$ = 30/60/10; 102 L/h; 50 mbar.	X_{CH4} = 87% at 700°C.	[41]
	2	SiC heating element (inside reactor) washcoated with Ni-based catalyst.	CH_4/H_2O/Ar = 1/3/7; GHSV = 182 $h^{-1.}$	X_{CH4} = 70% at 790°C.	[33]
	3	FeCrNi-alloy (inside reactor) coated with Ni-based catalyst.	$CH_4/H_2O/N_2$ = 1/3/2; GHSV = 157000 $cm^3/h/g_{cat.}$	X_{CH4} = 97% at 700°C.	[35]
	4	SiSiC foam (inside reactor) washcoated with Rh-based catalyst.	Catalyst density of 46 g/L; S/C = 4.1; GHSV = 150000 Nl/kg_{cat}/h.	X_{CH4} = 96% at 700 °C; Energy efficiency 61%; Specific energy 2.0 kWh/Nm^3_{H2}.	[44]
			Catalyst density of 86.3 g/L; S/C = 4.1; GHSV = 150000 Nl/kg_{cat}/h.	Almost full methane conversion above 700°C; Energy efficiency 81%; Specific energy 1.24 kWh/Nm^3_{H2}.	This work

the activation of the reaction. The cold-spot is located close to the inlet region, where the reaction is fast due the high concentration of the reactants. Then, rapidly, Joule heating is able to provide more heat than the one required by the reaction, with a consequent increase of the temperature until the outlet of the system. Correct design of inlet region and dosing of the thermal power is required to prevent the temperature from exceeding the maximum catalyst operative temperature and from crossing regions where carbon formation is possible.

Fig. 12 compares the experimental and numerically computed methane conversions and energy efficiencies as a function of the power input. In the case of the model, once the net enthalpy gain is equal to the experimental one, the power input is calculated with the current and the voltage resulting from the simulation. Then the energy efficiency is calculated including ohmic losses that correspond to 3% of the total input electric power: such losses were estimated based on the set current considering the length and size of the conductors whose resistivity was evaluated at 50°C. The model is able to match closely the methane conversion and the thermal efficiency recorded experimentally. The outlet temperature is also reasonably well predicted by the model.

Scale-up considerations

In this section, using the previously validated model, we design an intensified unit able to operate with industrial electric plugs (400 V, 650 A max). Experimental test results showed that the system can be operated at T > 700°C, S/C ≥ 3 and GHSV = 150000 Nl/h/kg_{cat} with a catalyst density of 86.3 g/L providing excellent catalytic performance (almost complete methane conversion) and high energy efficiency. We took these results as the basis of our scale-up evaluation, by setting proper values of steam-to-carbon, space velocity and catalyst inventory.

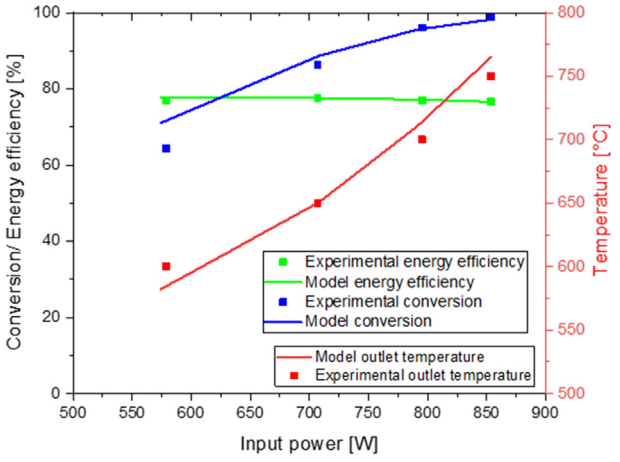

Fig. 12 – Comparison of experimental and simulated methane conversions, energy efficiencies, and outlet temperatures in intensified eMSR tests. Foam C, 1% Rh/Al_2O_3 washcoated (4/5) on SiSiC foam with a catalyst loading of 2.6 g, feed mixture of CH_4 and H_2O with steam to carbon ratio (S/C) of 4.1, gas hourly space velocity (GHSV) of 150000 Nl/h/kg_{cat}, ambient pressure.

The design was constrained considering a maximum operative temperature (800°C) and a maximum pressure drop (1 bar). Differently from the lab-scale configuration, it was assumed that such a unit is integrated in a H_2 production process, and that the feedstock undergoes first a desulphurization treatment. Therefore, the inlet temperature was set at 450°C, compatible with feed pre-treating units, which removes the requirement of a first portion of the reactor operating in heating-only mode. The outlet pressure was set to 7 bar, in accordance with the adoption of a pressure swing adsorption stage for H_2 separation, as reported by the HyGear research team, with a temperature of 800°C, close to the range of experimentally investigated conditions [83].

The foam specification considered for simulation was the same used in the experimental section, and the catalyst inventory was increased only by 15%, to reach 100 g/L. This still allows the system to operate with a minor impact of internal and external mass transfer limitations. In accordance with experimental tests, the space velocity was set to 150000 Nl/h/kg_{cat}, a value that, based on experimental evidence, allows to operate close to thermodynamic equilibrium at 750°C. Two S/C ratios, 3 and 4, respectively were considered. As discussed, a higher pressure will increase the rate of reaction, therefore this choice is conservative for operations close to the equilibrium. The foam length and diameter were varied to obtain the maximum H_2 productivity within the constraints on pressure drop, voltage and current. Firstly, different reactor geometries were considered (length and diameter) and then optimized values to meet the specifications listed above were calculated.

The outlet conversion granted by reactors with different diameters and lengths is almost constant (93.3% ± 0.1) since the system approaches thermodynamic equilibrium at 800°C with inlet S/C = 4. The H_2 production increases linearly with reactor length and quadratically with the reactor diameter. A reactor with a foam diameter of 11.75 cm and a total length of 1.75 m was able to meet all the constraints with a H_2 production of about 200 Nm^3/h, a target value *e.g.* for H_2 refilling stations. By looking at the effect of reactor length on the constraints, it was apparent that the constraint on the total ΔV is more stringent that on the pressure drops. Operating in these conditions leads to thermal efficiencies in excess of 97.5%, due to the large reactor diameter and insulant thickness considered for this application.

Performing the same analysis for a lower steam to carbon ratio (S/C = 3) leads to a marginal effect on the productivity and on other KPIs. In a slightly smaller reactor (1.7 m, 11.3 cm diameter) it is possible to produce 215 Nm^3/h of H_2 with almost the same thermal efficiency, which grows from 97.5 to 98%. Due to thermodynamic limitations, the methane conversion is slightly lower (89% vs 93%). A full process analysis is needed to identify the optimal operating conditions.

Conclusions

In this work, electrified methane steam reforming for low-carbon H_2 production was systematically studied in the case of the direct Joule heating of Rh/Al_2O_3 catalyst washcoated SiSiC foams, where the SiSiC foam serves as the catalyst

coating support as well as the resistive heating element. The washcoated SiSiC foams, electrically connected to a power generator, were investigated at different operating conditions, such as space velocity, operating pressure as well as under intensified conditions. Full methane conversion was achieved even at a high space velocity of 200000 Nl/h/kg_{cat} at temperatures above 650°C. These results suggest that a high space velocity exhibits a significant positive effect on the hydrogen productivity. The methane conversion and the hydrogen productivity were negatively affected by increasing the operating pressure; which however promoted the H_2 fraction in the produced syngas. Compared to the operating temperature and pressure, which both show a minor negative effect on the energy efficiency, incrementing the space velocity has a positive effect and plays an important role in promoting the overall energy efficiency. The heat losses grow almost linearly with the reactor temperature but are independent from the space velocity, so that the overall energy efficiency increases with increasing flow rate. A specific energy demand as low as 1.24 kWh/Nm^3_{H2} was achieved on a washcoated SiSiC foam with a catalyst density of 86.3 g/L (GHSV = 150000 Nl/h/kg_{cat}, S/C = 4.1, ambient pressure), because of an unprecedented high energy efficiency of 81%.

A previously developed mathematical model of the eMSR reactor has been herein validated against the experimental data, showing a very good agreement with the collected intensified results and serving as a useful tool for experiment design.

Preliminary scale-up calculations have been performed with the aim of designing a compact unit for H_2 production compatible with industrial electricity supply lines. We show that it is possible to design highly efficient small-scale eMSR units with hydrogen productivities up to 200 Nm^3/h.

By exploiting renewable electricity, the foam-based eMSR concept promises an important chance for mitigating CO_2 emissions. Notably, the same direct electrification concept is applicable in principle to other endothermic reactions, such as reverse water-gas shift reaction, dehydrogenations (*e.g.*, C_2H_6 to C_2H_4), NH_3 decomposition and other cracking reactions.

Declaration of competing interest

The authors declare that they have no known competing financial interests or personal relationships that could have appeared to influence the work reported in this paper.

Acknowledgments

This project has received funding from the European Research Council (ERC) under the European Union's Horizon 2020 research and innovation programme (GA No. 694910 -'INTENT'), and from the project "PLUG-IN" funded by the MIUR Progetti di Ricerca di Rilevante Interesse Nazionale (PRIN) Bando 2020. The authors thank Marco Roncato and Enrico Morandini for their assistance in the present work. The work of Federico Nicolini and Lotte Capel is acknowledged. Daniele Marangoni is gratefully acknowledged for technical support to the catalyst testing.

Appendix A. Supplementary data

Supplementary data to this article can be found online at https://doi.org/10.1016/j.ijhydene.2022.12.346.

REFERENCES

[1] Wang F, Harindintwali JD, Yuan Z, Wang M, Wang F, Li S, et al. Technologies and perspectives for achieving carbon neutrality. Innovation 2021:100180.
[2] Barreto L, Makihira A, Riahi K. The hydrogen economy in the 21st century: a sustainable development scenario. Int J Hydrogen Energy 2003;28:267–84.
[3] International Energy Agency. Global hydrogen review 2021. www.iea.org. [Accessed 6 July 2022].
[4] Chen L, Qi Z, Zhang S, Su J, Somorjai GA. Catalytic hydrogen production from methane: a review on recent progress and prospect. Catalysts 2020;10:858.
[5] IEA. The future of hydrogen. Paris: IEA; 2019. https://www.iea.org/reports/the-future-of-hydrogen. [Accessed 25 July 2022].
[6] Zhang H, Sun Z, Hu YH. Steam reforming of methane: current states of catalyst design and process upgrading. Renew Sustain Energy Rev 2021;149:111330.
[7] Meloni E, Martino M, Palma V. A short review on Ni based catalysts and related engineering issues for methane steam reforming. Catalysts 2020;10:352.
[8] Howarth RW, Jacobson MZ. How green is blue hydrogen? Energy Sci Eng 2021;9:1676–87.
[9] Holladay JD, Hu J, King DL, Wang Y. An overview of hydrogen production technologies. Catal Today 2009;139:244–60.
[10] Le Quéré C, Moriarty R, Andrew RM, Canadell JG, Sitch S, Korsbakken JI, et al. Global carbon budget 2015. Earth Syst Sci Data 2015;7:349–96.
[11] Balzarotti R, Beretta A, Groppi G, Tronconi E. A comparison between washcoated and packed copper foams for the intensification of methane steam reforming. Reaction Chemistry & Engineering 2019;4:1387–92.
[12] Balzarotti R, Ambrosetti M, Beretta A, Groppi G, Tronconi E. Investigation of packed conductive foams as a novel reactor configuration for methane steam reforming. Chem Eng J 2020;391:123494.
[13] Ambrosetti M, Bonincontro D, Balzarotti R, Beretta A, Groppi G, Tronconi E. H_2 production by methane steam reforming over Rh/Al_2O_3 catalyst packed in Cu foams: a strategy for the kinetic investigation in concentrated conditions. Catal Today 2022;387:107–18.
[14] Ashraf MA, Tacchino S, Peela NR, Ercolino G, Gill KK, Vlachos DG, et al. Experimental insights into the coupling of methane combustion and steam reforming in a catalytic plate reactor in transient mode. Ind Eng Chem Res 2020;60:196–209.
[15] Pourali M, Esfahani JA. Performance analysis of a micro-scale integrated hydrogen production system by analytical approach, machine learning, and response surface methodology. Energy 2022;255:124553.
[16] Pourali M, Esfahani JA, Sadeghi MA, Kim KC, Gostick J. Simulation of methane steam reforming in a catalytic microreactor using a combined analytical approach and response surface methodology. Int J Hydrogen Energy 2021;46:22763–76.

[17] Jahangir H, Esfahani JA, Pourali M, Kim KC. Parameter study of a porous solar-based propane steam reformer using computational fluid dynamics and response surface methodology. Int J Hydrogen Energy 2022;47:36465–81.
[18] Van Geem KM, Weckhuysen BM. Toward an e-chemistree: materials for electrification of the chemical industry. MRS Bull 2022:1–10.
[19] Gong J, English NJ, Pant D, Patzke GR, Protti S, Zhang T. Power-to-X: lighting the path to a net-zero-emission future. ACS Publications; 2021. p. 7179–81.
[20] Van Geem KM, Galvita VV, Marin GB. Making chemicals with electricity. Science 2019;364:734–5.
[21] Dong Q, Yao Y, Cheng S, Alexopoulos K, Gao J, Srinivas S, et al. Programmable heating and quenching for efficient thermochemical synthesis. Nature 2022;605:470–6.
[22] Stankiewicz AI, Nigar H. Beyond electrolysis: old challenges and new concepts of electricity-driven chemical reactors. Reaction Chemistry & Engineering 2020;5:1005–16.
[23] Gjorgievski VZ, Markovska N, Abazi A, Duić N. The potential of power-to-heat demand response to improve the flexibility of the energy system: an empirical review. Renew Sustain Energy Rev 2021;138:110489.
[24] Almind MR, Vendelbo SB, Hansen MF, Vinum MG, Frandsen C, Mortensen PM, et al. Improving performance of induction-heated steam methane reforming. Catal Today 2020;342:13–20.
[25] Ma J, Jiang B, Li L, Yu K, Zhang Q, Lv Z, et al. A high temperature tubular reactor with hybrid concentrated solar and electric heat supply for steam methane reforming. Chem Eng J 2022;428:132073.
[26] Varsano F, Bellusci M, La Barbera A, Petrecca M, Albino M, Sangregorio C. Dry reforming of methane powered by magnetic induction. Int J Hydrogen Energy 2019;44:21037–44.
[27] Scarfiello C, Bellusci M, Pilloni L, Pietrogiacomi D, La Barbera A, Varsano F. Supported catalysts for induction-heated steam reforming of methane. Int J Hydrogen Energy 2021;46:134–45.
[28] Meloni E, Martino M, Ricca A, Palma V. Ultracompact methane steam reforming reactor based on microwaves susceptible structured catalysts for distributed hydrogen production. Int J Hydrogen Energy 2021;46:13729–47.
[29] de Dios García I, Stankiewicz A, Nigar H. Syngas production via microwave-assisted dry reforming of methane. Catal Today 2021;362:72–80.
[30] Li L, Wang H, Jiang X, Song Z, Zhao X, Ma C. Microwave-enhanced methane combined reforming by CO_2 and H_2O into syngas production on biomass-derived char. Fuel 2016;185:692–700.
[31] Chen W, Malhotra A, Yu K, Zheng W, Plaza-Gonzalez PJ, Catala-Civera JM, et al. Intensified microwave-assisted heterogeneous catalytic reactors for sustainable chemical manufacturing. Chem Eng J 2021:130476.
[32] Marin CM, Popczun EJ, Nguyen-Phan T-D, Alfonso D, Waluyo I, Hunt A, et al. Designing perovskite catalysts for controlled active-site exsolution in the microwave dry reforming of methane. Appl Catal B Environ 2021;284:119711.
[33] Renda S, Cortese M, Iervolino G, Martino M, Meloni E, Palma V. Electrically driven SiC-based structured catalysts for intensified reforming processes. Catal Today 2022;383:31–43.
[34] Rieks M, Bellinghausen R, Kockmann N, Mleczko L. Experimental study of methane dry reforming in an electrically heated reactor. Int J Hydrogen Energy 2015;40:15940–51.
[35] Zhou L, Guo Y, Yagi M, Sakurai M, Kameyama H. Investigation of a novel porous anodic alumina plate for methane steam reforming: hydrothermal stability, electrical heating possibility and reforming reactivity. Int J Hydrogen Energy 2009;34:844–58.
[36] Balakotaiah V, Ratnakar RR. Modular reactors with electrical resistance heating for hydrocarbon cracking and other endothermic reactions. AIChE J 2022;68:e17542.
[37] Lu YR, Nikrityuk PA. Steam methane reforming driven by the Joule heating. Chem Eng Sci 2022;251:117446.
[38] Liu F, Zhao Z, Ma Y, Gao Y, Li J, Hu X, et al. Robust Joule-heating ceramic reactors for catalytic CO oxidation. Journal of Advanced Ceramics 2022:1–9.
[39] Staff IEA. World energy statistics 2017. OECD; 2017.
[40] Song H, Liu Y, Bian H, Shen M, Lin X. Energy, environment, and economic analyses on a novel hydrogen production method by electrified steam methane reforming with renewable energy accommodation. Energy Convers Manag 2022;258:115513.
[41] Wismann ST, Engbæk JS, Vendelbo SB, Bendixen FB, Eriksen WL, Aasberg-Petersen K, et al. Electrified methane reforming: a compact approach to greener industrial hydrogen production. Science 2019;364:756–9.
[42] Delikonstantis E, Igos E, Theofanidis S-A, Benetto E, Marin GB, Van Geem K, et al. An assessment of electrified methanol production from an environmental perspective. Green Chem 2021;23:7243–58.
[43] Mion A, Galli F, Mocellin P, Guffanti S, Pauletto G. Electrified methane reforming decarbonises methanol synthesis. J CO2 Util 2022;58:101911.
[44] Zheng L, Ambrosetti M, Marangoni D, Beretta A, Groppi G, Tronconi E. Electrified methane steam reforming on a washcoated SiSiC foam for low-carbon hydrogen production. AIChE J 2023;69:e17620. https://doi.org/10.1002/aic.17620.
[45] Natrella G, Borgogna A, Salladini A, Iaquaniello G. How to give a renewed chance to natural gas as feed for the production of hydrogen: electric MSR coupled with CO_2 mineralization. Cleaner Engineering and Technology 2021:100280.
[46] Jovan DJ, Dolanc G. Can green hydrogen production be economically viable under current market conditions. Energies 2020;13:6599.
[47] Wismann ST, Engbæk JS, Vendelbo SB, Eriksen WL, Frandsen C, Mortensen PM, et al. Electrified methane reforming: understanding the dynamic interplay. Ind Eng Chem Res 2019;58:23380–8.
[48] Wismann ST, Engbæk JS, Vendelbo SB, Eriksen WL, Frandsen C, Mortensen PM, et al. Electrified methane reforming: elucidating transient phenomena. Chem Eng J 2021;425:131509.
[49] Wang Q, Ren Y, Kuang X, Zhu D, Wang P, Zhang L. Electrically heated monolithic catalyst for in-situ hydrogen production by methanol steam reforming. Int J Hydrogen Energy 2023;48:522–4.
[50] Bracconi M, Ambrosetti M, Maestri M, Groppi G, Tronconi E. A fundamental analysis of the influence of the geometrical properties on the effective thermal conductivity of open-cell foams. Chemical Engineering and Processing-Process Intensification 2018;129:181–9.
[51] Bracconi M, Ambrosetti M, Maestri M, Groppi G, Tronconi E. A fundamental investigation of gas/solid mass transfer in open-cell foams using a combined experimental and CFD approach. Chem Eng J 2018;352:558–71.
[52] Italiano C, Ferrante GD, Pino L, Laganà M, Ferraro M, Antonucci V, et al. Silicon carbide and alumina open-cell foams activated by Ni/CeO_2-ZrO_2 catalyst for CO_2 methanation in a heat-exchanger reactor. Chem Eng J 2022:134685.
[53] Dou L, Yan C, Zhong L, Zhang D, Zhang J, Li X, et al. Enhancing CO_2 methanation over a metal foam structured catalyst by electric internal heating. Chem Commun 2020;56:205–8.

[54] Dou L, Fu M, Gao Y, Wang L, Yan C, Ma T, et al. Efficient sulfur resistance of Fe, La and Ce doped hierarchically structured catalysts for low-temperature methanation integrated with electric internal heating. Fuel 2021;283:118984.
[55] Badakhsh A, Kwak Y, Lee Y-J, Jeong H, Kim Y, Sohn H, et al. A compact catalytic foam reactor for decomposition of ammonia by the Joule-heating mechanism. Chem Eng J 2021:130802.
[56] Ambrosetti M, Beretta A, Groppi G, Tronconi E. A numerical investigation of electrically-heated methane steam reforming over structured catalysts. Frontiers in Chemical Engineering 2021;3:747636.
[57] Pelanconi M, Bianchi G, Colombo P, Ortona A. Fabrication of dense SiSiC ceramics by a hybrid additive manufacturing process. J Am Ceram Soc 2022;105:786–93.
[58] Ambrosetti M, Bracconi M, Groppi G, Tronconi E. Analytical geometrical model of open cell foams with detailed description of strut-node intersection. Chem Ing Tech 2017;89:915–25.
[59] Sharma A, Rani RU, Malek A, Acharya K, Muddu M, Kumar S. Black anodizing of a magnesium-lithium alloy. Met Finish 1996;94:16–27.
[60] Bracconi M, Ambrosetti M, Okafor O, Sans V, Zhang X, Ou X, et al. Investigation of pressure drop in 3D replicated open-cell foams: coupling CFD with experimental data on additively manufactured foams. Chem Eng J 2019;377:120123.
[61] Gangurde LS, Sturm GS, Devadiga TJ, Stankiewicz AI, Stefanidis GD. Complexity and challenges in noncontact high temperature measurements in microwave-assisted catalytic reactors. Ind Eng Chem Res 2017;56:13379–91.
[62] Gangurde LS, Sturm GS, Valero-Romero M, Mallada R, Santamaria J, Stankiewicz AI, et al. Synthesis, characterization, and application of ruthenium-doped $SrTiO_3$ perovskite catalysts for microwave-assisted methane dry reforming. Chemical Engineering and Processing-Process Intensification 2018;127:178–90.
[63] Pelissier K, Chartier T, Laurent J. Silicon carbide heating elements. Ceram Int 1998;24:371–7.
[64] Kumar A, Baldea M, Edgar TF. A physics-based model for industrial steam-methane reformer optimization with non-uniform temperature field. Comput Chem Eng 2017;105:224–36.
[65] Lee B, Lim H. Cost-competitive methane steam reforming in a membrane reactor for H_2 production: technical and economic evaluation with a window of a H_2 selectivity. Int J Energy Res 2019;43:1468–78.
[66] Oyama ST, Hacarlioglu P, Gu Y, Lee D. Dry reforming of methane has no future for hydrogen production: comparison with steam reforming at high pressure in standard and membrane reactors. Int J Hydrogen Energy 2012;37:10444–50.
[67] Van Hook JP. Methane-steam reforming. Catal Rev Sci Eng 1980;21:1–51.
[68] Murkin C, Brightling J. Eighty years of steam reforming. Johnson Matthey Technology Review 2016;60:263–9.
[69] Kaiwen L, Bin Y, Tao Z. Economic analysis of hydrogen production from steam reforming process: a literature review. Energy Sources B Energy Econ Plann 2018;13:109–15.
[70] Bicer Y, Khalid F. Life cycle environmental impact comparison of solid oxide fuel cells fueled by natural gas, hydrogen, ammonia and methanol for combined heat and power generation. Int J Hydrogen Energy 2020;45:3670–85.
[71] Uemiya S. Brief review of steam reforming using a metal membrane reactor. Top Catal 2004;29:79–84.
[72] Uemiya S, Sato N, Ando H, Matsuda T, Kikuchi E. Steam reforming of methane in a hydrogen-permeable membrane reactor. Appl Catal 1990;67:223–30.
[73] Jørgensen SL, Nielsen PH, Lehrmann P. Steam reforming of methane in a membrane reactor. Catal Today 1995;25:303–7.
[74] Zheng L, Li H, Yu H, Kang G, Xu T, Yu J, et al. Modified" liquid–liquid displacement porometry and its applications in Pd-based composite membranes. Membranes 2018;8:29.
[75] Zheng L, Li H, Xu T, Bao F, Xu H. Defect size analysis approach combined with silicate gel/ceramic particles for defect repair of Pd composite membranes. Int J Hydrogen Energy 2016;41:18522–32.
[76] Sprung C, Arstad B, Olsbye U. Methane steam reforming over Ni/NiAl2O4 catalyst: the effect of steam-to-methane ratio. Top Catal 2011;54:1063–9.
[77] Yamazaki O, Tomishige K, Fujimoto K. Development of highly stable nickel catalyst for methane-steam reaction under low steam to carbon ratio. Appl Catal Gen 1996;136:49–56.
[78] Wang Y, Chin Y-H, Rozmiarek RT, Johnson BR, Gao Y, Watson J, et al. Highly active and stable Rh/MgO-Al_2O_3 catalysts for methane steam reforming. Catal Today 2004;98:575–81.
[79] Pérez-Camacho MN, Abu-Dahrieh J, Rooney D, Sun K. Biogas reforming using renewable wind energy and induction heating. Catal Today 2015;242:129–38.
[80] Meloni E, Martino M, Palma V. Microwave assisted steam reforming in a high efficiency catalytic reactor. Renew Energy 2022;197:893–901.
[81] Mortensen PM, Engbæk JS, Vendelbo SB, Hansen MF, Østberg M. Direct hysteresis heating of catalytically active Ni–Co nanoparticles as steam reforming catalyst. Ind Eng Chem Res 2017;56:14006–13.
[82] Vinum MG, Almind MR, Engbæk JS, Vendelbo SB, Hansen MF, Frandsen C, et al. Dual-function cobalt–nickel nanoparticles tailored for high-temperature induction-heated steam methane reforming. Angew Chem 2018;130:10729–33.
[83] Moneti M, Di Carlo A, Bocci E, Foscolo P, Villarini M, Carlini M. Influence of the main gasifier parameters on a real system for hydrogen production from biomass. Int J Hydrogen Energy 2016;41:11965–73.